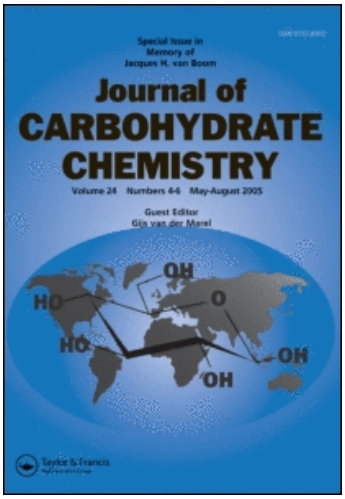

Journal of Carbohydrate Chemistry

Publication details, including instructions for authors and subscription information:
http://www.informaworld.com/smpp/title~content=t713617200

High and Low Energy FAB Tandem Mass Spectrometry of a Series of Anomeric and Regioisomeric 2'-Deoxyribofuranosyl Imidazole Nucleosides

J. H. Banoub[ab]; M. Becchi[c]; G. Descotes[b]; D. Fraisse[c]; R. W. Humble[d]; G. Mackenzie[bd]
[a] Department of Fisheries and Oceans, Science Branch, Canada [b] Laboratoire de Chimie Organique, Universite Claude Bernard Lyon, Villeurbanne Cedex, France [c] SCA-CNRS, Vernaison, France [d] Humberside Polytechnic, Hull, U.K.

To cite this Article Banoub, J. H. , Becchi, M. , Descotes, G. , Fraisse, D. , Humble, R. W. and Mackenzie, G.(1992) 'High and Low Energy FAB Tandem Mass Spectrometry of a Series of Anomeric and Regioisomeric 2'-Deoxyribofuranosyl Imidazole Nucleosides', Journal of Carbohydrate Chemistry, 11: 4, 471 — 484
To link to this Article: DOI: 10.1080/07328309208017807
URL: http://dx.doi.org/10.1080/07328309208017807

J. CARBOHYDRATE CHEMISTRY, 11(4), 471-484 (1992)

HIGH AND LOW ENERGY FAB TANDEM MASS SPECTROMETRY OF A SERIES OF ANOMERIC AND REGIOISOMERIC 2'-DEOXYRIBOFURANOSYL IMIDAZOLE NUCLEOSIDES

J.H. Banoub,[1,2] M.Becchi,[3] G.Descotes,[2] D. Fraisse,[3]
R.W. Humble[4] and G. Mackenzie[2,4]

[1]Department of Fisheries and Oceans, Science Branch, P.O. Box 5667, St.John's, N.F., A1C 5X1, CANADA.
[2]Universite Claude Bernard Lyon, Laboratoire de Chimie Organique, URA CNRS 463, 43 Bd du 11 Novembre 1918, 69622 Villeurbanne, Cedex, France.
[3]SCA-CNRS, P.B.22, 69390 Vernaison, France.
[4]Humberside Polytechnic, Hull, HU6 7RT, U.K.

Received April 16, 1991 - Final Form January 15, 1992

ABSTRACT

Positive ion fast atom bombardment mass spectrometry has aided the structural characterisation of a novel series of anomeric and regioisomeric ethyl 5- and 4-amino-2'-deoxy-**D**-*erythro*-pentofuranosylimidazole-4- and 5 carboxylate nucleosides. Daughter ion MS/MS analyses (high energy MIKE and low energy MS/MS CAD), of the precursor protonated molecular ions for this series of anomeric and regioisomeric nucleosides have provided distinct and reproducible fingerprint patterns which have permitted discrimination between the individual configurations of the various anomers and regioisomers.

INTRODUCTION

5-Aminoimidazole nucleotides are of fundamental importance and occur in all living systems as intermediates in the *de novo* biosynthesis of purine

nucleotides as precursors to nucleic acids.[1] As part of a programme[2] aimed at the synthesis of inhibitors of enzymes within this pathway the novel nucleosides ethyl 5-amino-2′-deoxy-ß- and α-**D**-*erythro*-pentofuranosylimidazole-4-carboxylate [ß-N_1 (**1**) and α-N_1 (**3**) respectively] and ethyl 4-amino-2′-deoxy-ß- and α-**D**-*erythro*-pentofuranosylimidazole-5-carboxylates [ß-N_3(**2**) and α-N_3(**4**), respectively] were prepared and converted into 2′-deoxyribofuranosyl analogues of the pathway intermediate 5-amino-1-ß-**D**-ribofuranosylimidazole-4-carboxylic acid 5′-*O*-phosphate (CAIR).[3]

To date, no fast atom bombardment (FAB) mass spectrometric data have been reported for this series of 2′-deoxyribofuranosyl imidazole nucleosides. As a continuation of our interest in the study and differentiation of anomeric acyclic nucleosides,[4,5] **C**-glycosides, [6,7] disaccharide and bacterial antigens [8,9] and 1,2- *trans* - 2-deoxy-2-iodoglycosyl azides [10] by FAB MS and FAB tandem mass spectrometry, we now report on this series of synthetic 2′-deoxyribofuranosylimidazole nucleosides (**1-4**) and on two of their protected derivatives, namely : ethyl 5-amino-(2′-deoxy-3′, 5′-di-*O*-*p*-toluoyl)-ß-**D**-*erythro* pentofuranosylimidazole-4-carboxylate [ß-N_1 (**5**)] and ethyl 4-amino-(2′-deoxy-3′,5′-di-*O*-*p*-toluoyl)-ß-**D**-*erythro*-pentofuranosylimidazole-5-carboxylate [ß-N_3 (**6**)].

RESULTS AND DISCUSSION

The positive ion FAB mass spectra of the series of anomeric and regioisomeric 2′-deoxyribofuranosyl imidazole nucleosides (**1** - **4**), were recorded and the data for the more characteristic ions are presented in Table 1. The FAB mass spectra were very similar for the four isomers (**1** - **4**). As expected, all the nucleosides formed the respective protonated molecules $[M+H]^+$ and the matrix adducts $[G+M+H]^+$ at m/z 272 and 364 respectively. These peaks permitted the determination of the relative molecular masses. The characteristic fragment ions appeared to be the same for all the four isomers. The fragmentation patterns of the protonated molecules $[M+H]^+$ followed

TABLE 1. Positive ion fast atom bombardment mass spectrometry of the regioisomeric ß-N_1 (**1**) and ß-N_3 (**2**) 5-amino- and 4-amino-imidazole-2′-deoxy-nucleosides and their respective anomers α-N_1 (**3**) and α-N_3 (**4**)

		C_{11} H_{17} N_3 O_5 (MW 271)			
Characteristic Ions	m/z	ß-N_1(**1**) (%)	ß-N_3(**2**) (%)	α-N_1(**3**) (%)	α-N_3(**4**) (%)
$[2M+Na]^+$	543	(17)	(3)	(-)	(-)
$[G+M+H]^+$	364	(14)	(19)	(5)	(6)
$[M+H]^+$	272	(100)	(97)	(41)	(56)
$[MH-90]^+$ or $[S_1+H]^+$	182	(3)	(25)	(6)	(5)
$[BH_2]^+$	156	(98)	(100)	(100)	(100)
$[S]^+$	117	(24)	(12)	(40)	(12)
$[BH_2$-Et0H$]^+$	110	(26)	(22)	(50)	(28)

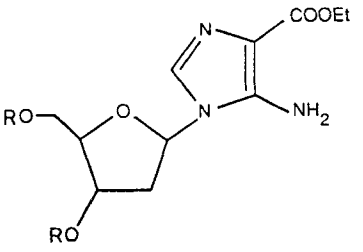

β-N_1

1 R = H
5 R= MePhCO (toluoyl)

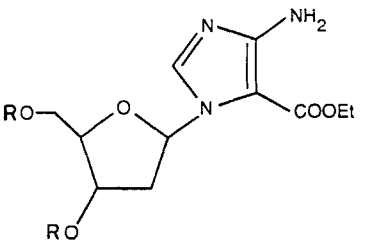

β-N_3

2 R = H
6 R=MePhCO (toluoyl)

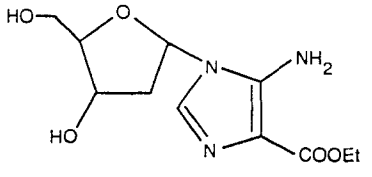

α-N_1
3

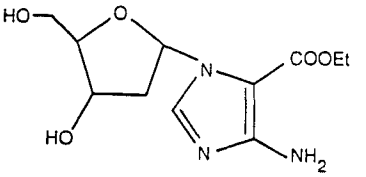

α-N_3
4

SCHEME 1

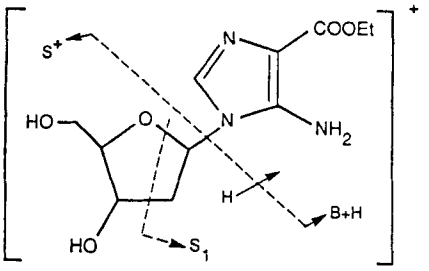

[s]$^+$=glycosyl portion = [MH-BH]$^+$=M/Z 117

[BH_2]$^+$=m/z 156

[S_1+H]=[MH-90]$^+$=m/z 182

processes which are analogous to the ones described by Crow *et al.*,[11] which appear to be initiated by the intramolecular transfer of a hydrogen atom from the sugar to the base, which is already protonated, (Scheme 1) to afford the $[BH_2]^+$ fragment-ion at m/z 156 (which is the base peak in the majority of cases). Other less abundant fragment ions were produced by the cleavage of the base-sugar bond with charge retention on the sugar moiety (A-type cleavage[12]) to afford the $[S]^+$ fragment-ion at m/z 117. The fragment-ion observed at m/z 110 corresponds to a loss of a molecule of ethanol from the $[BH_2]^+$ ion which can be accounted for by the following mechanism :

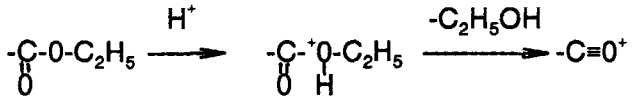

We also noticed that the fragment-ion at m/z 182, known as the $[S_1+H]^+$ fragment-ion,[12] was produced by the loss of $(C_3H_6O_3)$ 90 amu from the $[M+H]^+$ ion.

High energy CAD MS/MS experiments were carried out to obtain further information on fragmentations of ions formed from this series of regioisomeric and anomeric nucleosides. The $[M+H]^+$ ions at m/z 272 were selected for the recording of the unimolecular mass analysed ion kinetic energy (MIKE) and collision - activated dissociation mass analysed ion kinetic energy (CAD-MIKE) spectra. High energy CAD MS/MS spectra of positive ions often carry much more information than the positive FAB spectra. However, one of the main benefits of the MS/MS technique, is that all uncertainties concerning the origin of the fragment-ion are removed.

The MIKE and CAD-MIKE metastable analyses of the precursor ions $[M+H]^+$ at m/z 272 are summarised in Table 2. Examination of Table 2 permitted the fate of the $[M+H]^+$ between parent ions and their dissociations to be deduced. Comparison between these data, showed that for the two regioisomeric pairs ß-N_1 (**1**) and ß-N_3 (**2**), and, α-N_1 (**3**) and α-N_1 (**4**), little information could be obtained from the MIKE spectra. Within each respective

TABLE 2. MIKE and CAD-MIKE spectra of the precursor ions $[M+H]^+$ at m/z 272 obtained from the regioisomeric ethyl 5- and 4-amino-2'-deoxy-ß-**D**-*erythro*-pentofuranosylimidazol-4-and 5-carboxylate (**1**) and (**2**) and their respective α-anomers (**3**) and (**4**).

Daughter Ions	m/z	MIKE				CAD - MIKE			
		ß-N_1(**1**) (%)	ß-N_3(**2**) (%)	α-N_1(**3**) (%)	α-N_1(**4**) (%)	ß-N_1(**1**) (%)	ß-N_3(**2**) (%)	α-N_1(**3**) (%)	α-N_3(**4**) (%)
$[MH-NH_2]^+$	256	(-)	(-)	(7)	(12)	(-)	(-)	(4)	(-)
$[MH-NH_2-H_2O]^+$	238	(-)	(-)	(13)	(4)	(-)	(-)	(10)	(-)
$[MH-EtOH]^+$	226	(1)	(4)	(-)	(1)	(3)	(8)	(6)	(4)
$[MH-90]^+$	182	(-)	(-)	(-)	(-)	(6)	(4)	(9)	(7)
$[BH_2]^+$	156	(100)	(100)	(100)	(100)	(100)	(100)	(100)	(100)
$[MH-90-EtOH]^+$	136	(-)	(-)	(-)	(-)	(2)	(-)	(6)	(-)
$[S]^+$	117	(-)	(-)	(-)	(-)	(6)	(-)	(9)	(4)
$[BH_2-EtOH]^+$	110	(-)	(-)	(-)	(-)	(9)	(-)	(11)	(13)

part, the MIKE spectra were almost identical. However, the MIKE spectra permitted the differentiation between the respective anomeric pairs ß-N_1(**1**) and α-N_1(**3**), and, ß-N_3(**2**) and α-N_3(**4**). In effect, we noticed that the α-anomers **3** and **4** exhibited the exclusive presence of the diagnostic fragment-ions $[MH-NH_2]^+$ and $[MH-NH_2-H_2O]^+$ at m/z 256 and 238 respectively, which were absent in the MIKE spectra of the ß-anomers **1** and **2**.

The CAD-MIKE metastable analyses permitted differentiation among these four isomeric nucleosides. Thus comparison between the CAD-MIKE spectra of the regioisomeric nucleoside pair ß-N_1(**1**) and ß-N_3(**2**) showed pronounced differences. In effect, we observed that in the spectrum of the ß-N_1(**1**) regioisomer there was the presence of the diagnostic fragment-ions $[MH-90-EtOH]^+$, $[S]^+$ and $[BH_2-EtOH]$ at m/z 136, 117 and 110 respectively, which were absent in the case of the ß-N_3(**2**) regioisomer. Similarly, for the α-N_1(**3**) and α-N_3(**4**) regioisomeric pair, we observed that in the CAD-MIKE spectrum of α-N_1(**3**), there was the exclusive presence of the diagnostic fragment-ions $[MH-NH_2]^+$, $[MH-NH_2-H_2O]^+$ and $[MH-90-EtOH]^+$ at m/z 256, 238 and 136 respectively, which were absent in the spectrum of the α-N_3(**4**) regioisomer. Comparison between the CAD-MIKE analyses of the ß-N_1(**1**) and α-N_1(**3**) anomeric pair showed the exclusive presence of the diagnostic fragment-ions $[MH-NH_2]^+$ and $[MH-NH_2-H_2O]^+$ at m/z 256 and 238 respectively for the α-anomer **3**, whereas for the ß-N_3(**2**) and α-N_3(**4**) anomeric pair we noticed the exclusive presence of the diagnostic fragment-ions $[S]^+$ and $[BH_2-EtOH]^+$ at m/z 117 and 110 respectively for the α-anomer **4**.

Low energy CAD analyses were also carried out on the $[M+H]^+$ protonated molecular ion of the regioisomeric pair of the 2′-deoxyribofuranosyl imidazole nucleosides ß-N_1(**1**) and ß-N_3(**2**): shown in Table 3. The hybrid MS/MS analyses, performed with different collision energies 80eV and 150eV showed pronounced differences in the intensities of some fragment-ions, which permitted discrimination between these two regioisomers. It is worthwhile

TABLE 3. Low energy CAD analyses (MS/MS hybrid) of the $[M+H]^+$ precursor ions at m/z 272 obtained from the regioisomeric ethyl 5- and 4-amino-2′-deoxy-β-**D**-*erythro*-pentofuranosylimidazole-4- and 5-carboxylates (**1**) and (**2**)

Daughter-Ions	m/z	β-N_1(**1**)	β-N_3(**2**) 40eV	β-N_1(**1**)	β-N_3(**2**) 80eV	β-N_1(**2**)	β-N_3(**2**) 150eV
$[MH-NH_2]^+$	256	-	-	27	7	-	-
$[MH-H_2O]^+$	254	-	-	14	20	-	-
$[MH-CH_2OH]^+$	240	-	-	6	1	-	-
$[MH-90]^+$	182	-	-	-	1	-	-
$[BH_2]^+$	156	100	100	100	100	100	100
$[MH-90-EtOH]^+$	136	-	-	-	-	4	-
$[S]^+$	117	-	-	40	8	36	10
$[BH_2-EtOH]^+$	110	-	-	20	23	24	26
$[S-H_2O]^+$	99	-	-	9	2	13	14

pointing out that the hybrid MS/MS analyses, performed with a collision energy of 40eV, gave the same identical fragment-ion $[BH_2]^+$ at m/z 156 (base peak).

In effect, comparison between the hybrid MS/MS analyses performed with a collision energy 80eV, showed pronounced differences in the relative intensities of the fragment-ions $[MH-NH_2]^+$, $[S]^+$ and $[S-H_2O]^+$ at m/z 256, 117, and 99 respectively, which proved to be of diagnostic value in permitting discrimination between the ß-N_1(**1**) and ß-N_3(**2**) regioisomers. The hybrid MS/MS analysis performed at 150eV showed the presence of the diagnostic fragment-ion $[MH-90-EtOH]^+$ at m/z 136 and the pronounced differences in the relative intensities of the fragmentations $[S]^+$ and $[S-H_2O]^+$ at m/z 117 and 99 respectively, which allowed discrimination to be made between these two regioisomers.

The positive ion FAB mass spectra of ethyl 5-amino-(2′-deoxy-3′,5′-di-*O*-*p*-toluoyl)-ß-**D**-*erythro*-pentofuranosylimidazole-4-carboxylate (**5**) and ethyl 4-amino-(2′-deoxy-3′,5′-di-*O*-*p*-toluoyl)-ß-**D**-*erythro*-pentofuranosylimidazole-5-carboxylate (**6**) is also presented in Table 4. The FAB MS of these two regioisomers were very similar, and as expected we noticed the protonated molecules $[M+H]^+$ and the cationised molecules $[M+Na]^+$ at m/z 508 and 530 respectively. These peaks permitted the determination of the relative molecular masses. The characteristic fragment-ions appeared to be the same for these two regioisomers. We also noticed the presence of the toluoyl fragment-ion $[CH_3\phi CO]^1$ at m/z 119.

High and low energy CAD MS/MS experiments were performed to obtain further information on the fragmentation of the $[M+H]^+$ ion precursor at m/z 508 formed from this series of regioisomeric nucleosides. The MIKE, CAD-MIKE and hybrid MS/MS analyses performed at two different collision energies 50eV and 100eV, for the $[M+H]^+$ precursor ions are summarised in Table 5. Comparison between these data showed that discrimination between these two regioisomers **5** and **6** could be easily identified. In the case of the unimolecular MIKE analyses we could see pronounced differences in the relative

TABLE 4. Positive ion fast atom bombardment mass spectrometry of the regioisomeric ethyl 5- and 4- (2′-deoxy-3′,5′-di-*O*-p-toluoyl)-ß-**D**-*erythro*-pentofuranosylimidazole-4- and 5-carboxylates (**5**) and (**6**)

		$C_{27}H_{29}N_3O_7$ (MW 507)	
Characteristic Ions	m/z	ß-N_1(**5**) (%)	ß-N_3(**6**) (%)
$[M-Na]^+$	530	(27)	(5)
$[M+H]^+$	508	(72)	(14)
$[S]^+$	353	(32)	(15)
$[BH_2]^+$	156	(70)	(100)
$[MePhCO]^+$	119	(100)	(75)
$[BH_2\text{-EtOH}]^+$	110	(21)	(20)

TABLE 5. MIKE, CAD-MIKE and MS/MS hybrid analyses of the precursor ions $[M+H]^+$ at m/z 508 obtained from the regioisomeric ethyl 5- and 4-amino-(2′-deoxy-3′, 5′-di-*O*-*p*-toluoyl)-β-**D**-*erythro*- pentofuranosylimidazole-4- and 5-carboxylates (**5**) and (**6**)

Daughter Ions		MIKE		CAD-MIKE		MS/MS hybrid			
	m/z	β-N_1(**5**) (%)	β-N_3(**6**) (%)	β-N_1(**5**) (%)	β-N_3(**6**) (%)	β-N(**5**) (%)	β-N_3(**6**) (%)	β-N_3(**5**) (%)	β-N_1(**6**) (%)
						50eV		100eV	
$[MH-EtOH]^+$	462	(-)	(-)	(2)	(7)	(-)	(-)	(-)	(-)
$[MH-MePhCHO]^+$	388	(-)	(-)	(5)	(6)	(-)	(-)	(-)	(-)
$[MH-MePhCOOH]^+$	372	(32)	(100)	(27)	(36)	(9)	(8)	(4)	(2)
$[S]^+$	353	(100)	(45)	(100)	(100)	(49)	(15)	(28)	(9)
$[NH-2MePhCOOH]^+$	236	(-)	(-)	(-)	(-)	(-)	(-)	(10)	(-)
$[BH_2]^+$	156	(2)	(29)	(13)	(85)	(25)	(100)	(36)	(100)
$[MePhCO]^+$	119	(-)	(-)	(7)	(15)	-	-	(3)	(-)
$[BH_2\text{-}EtOH]^+$	110	(-)	(-)	(-)	(8)	-	-	(10)	(-)

abundances of the fragment-ions $[MH\text{-}MePhCOOH]^+$, $[S]^+$ and $[BH_2]^+$ at m/z 372, 353 and 156 respectively. In the case of the CAD-MIKE analyses, we could observe the presence of the diagnostic fragment-ion $[BH_2\text{-}EtOH]^+$ at m/z 110 for the regioisomer **6**, and pronounced differences in the relative abundances of the $[BH_2]^+$ ion at m/z 156. The hybrid MS/MS analyses, performed at a collision energy of 50eV also showed pronounced differences of the relative intensities of all fragment-ions present. Finally the hybrid MS/MS analyses performed at a collision energy of 100eV showed two distinct and discriminating fingerprint ion patterns, which permitted differentiation between these two regioisomers.

It is interesting to mention that one of the earliest uses of tandem mass spectrometry (MS/MS) for biochemical analyses was in the study of nucleosides and nucleotides.[12,13,14] Daughter ion MS/MS spectra generated by the use of fast atom bombardment ionisation permitted the distinction between isomeric sequences in both the ribo- and deoxyribonucleotides, cyclic nucleosides, and also positional isomers of nucleosides and nucleotides.

The present MS/MS results appeared to be consistent with the sequential mass spectra of substituted nebularine and tubercidin nucleosides.[11]

CONCLUSION

Positive ion FAB mass spectrometry and tandem mass spectrometry permitted differentiation between the members of this series of synthetic anomeric and regioisomeric 2′-deoxyribofuranosyl imidazole nucleosides. The high and low energy MS/MS analyses of the protonated molecular ions $[M+H]^+$, as precursors, provided reproducible discriminating fingerprints. These patterns reflect the inequalities of the chemical free energy and the stereochemical differences of the substituents located on C-4 and C-5 of the imidazole base, and of the anomeric configurations of C-1′ of the 2-deoxyribose position, which contribute to the differences in the tertiary structures[16] of the protonated-molecular ions studied. The distinct fingerprint

patterns permitted discrimination between the individual anomers and regioisomers.

EXPERIMENTAL

All analyses were performed on a VG ZAB2-SEQ mass spectrometer (VG Analytical, Manchester, UK) with a BEqQ design. Ionisation was by liquid-assisted secondary ion mass spectrometry (LSI MS), using cesium ions of approximately 35KeV energy. For each compound a dichloromethane solution was added to the matrix (glycerol).

Collision activated decomposition-mass analysed kinetic energy (CAD-MIKE) analyses were performed using helium as a collision gas, to give attenuation of the precursor ion intensity of approximately 80%. The laboratory collision energy was 8KeV. The helium pressure in the collision cell was adjusted until the main ion beam was reduced by a factor of five. Low energy collision activated decomposition analyses were performed by collision with argon in the first quadrupole, at a pressure yielding approximately 50% attenuation of the intensity of the precursor ion. Collision energies were 50 and 100eV.

REFERENCES

1. J. M. Buchanan and S. C. Hartman, *Advan. Enzymol.*, **21**, 199 (1959).

2. G. Mackenzie, R. W. Humble, D. F. Ewing, A. Holy, I. Votruba and G. Shaw, *Nucleosides & Nucleotides*, **8**, 177 (1989).

3. G. Mackenzie, R. W. Humble, D. F. Ewing, A. Holy, I. Votruba, G. Shaw and F. Hewedi, *Carbohydr. Res.*, **216**, 109 (1991).

4. J. H. Banoub, G. Mackenzie, M. Becchi, D. Fraisse and G. Descotes, *Spectros. Int. J.*, **7**, 331 (1989).

5. J. H. Banoub, G. Mackenzie, G. Descotes, R. W. Humble, G. Shaw, M. Becchi and D. Fraisse, *Biomed. Environ. Mass Spectrom.*, **19**, 97 (1990).

6. M. Brakta, P. Lhoste, D. Sinou and J. H. Banoub, *Carbohydr. Res.*, **203**, 148 (1990).

7. M. Brakta, P. Lhoste, D. Sinou, M. Becchi, D. Fraisse and J. H. Banoub, *Org. Mass Spectrom.*, **25**, 249 (1990).

8. J. H. Banoub, P. Boullanger, C. Andre, M. Becchi and D. Fraisse, *Org. Mass Spectrom.*, **25**, 129 (1990).

9. J. H. Banoub, D. H. Shaw, H. Pang, J. J. Krepinsky, N. S. Nakhla and T. R. Patel, *Biomed. Environ. Mass Spectrom.*, **19**, 787 (1990).

10. J. H. Banoub, M. Becchi, D. Lafont, D. Fraisse and G. Descotes, *Rapid Commun. Mass Spectrom.*, **4**, 536 (1990).

11. F. W. Crow, K. B. Tomer, M. L. Gross, J. A. McCloskey and D. E. Bergstrom, *Anal. Biochem.*, **139**, 243 (1984).

12. K. L. Busch, G. L. Glish and S. A. McLuckey, *Mass Spectrometry/ Mass Spectrometry. Techniques and Applications of Tandem Mass Spectrometry.* VCH Publishers Inc., New York, 1988, p 217.

13. B. Kralj, V. Kramer, R. Susic and J. Krobe, *Biomed. Mass Spectrom.*, **12**, 673 (1985).

14. P. F. Crain, *Mass Spectrom. Rev.*, **9**, 505 (1990).